

Deep Clustering based Boundary-Decoder Net for Inter and Intra Layer Stress Prediction of Heterogeneous Integrated IC Chip

Kart Leong Lim, Ji Lin

Institute of Microelectronics (IME),

Agency for Science, Technology and Research (A*STAR),

2 Fusionopolis Way, Innovis #08-02, Singapore 138634, Republic of Singapore

{limkl, ji_lin}@ime.a-star.edu.sg

Abstract—High stress occurs when 3D heterogeneous IC packages are subjected to thermal cycling at extreme temperatures. Stress mainly occurs at the interface between different materials. We investigate stress image using latent space representation which is based on using deep generative model (DGM). However, most DGM approaches are unsupervised, meaning they resort to image pairing (input and output) to train DGM. Instead, we rely on a recent boundary-decoder (BD) net, which uses boundary condition and image pairing for stress modeling. The boundary net maps material parameters to the latent space co-shared by its image counterpart. Because such a setup is dimensionally wise ill-posed, we further couple BD net with deep clustering. To access the performance of our proposed method, we simulate an IC chip dataset comprising of 1825 stress images. We compare our new approach using variants of BD net as well as a baseline approach. We show that our approach is able to outperform all the comparison in terms of train and test error reduction.

I. INTRODUCTION

Advanced packaging of IC chips [1], [2], [3], [4] involves complex heterogeneous integration. The integration between different structures and materials, e.g. die, UF and RDL, inside IC chips, is prone to fracture when subjected to thermal cycling [5], [6], [7], [8], [9], [10]. Stress prediction [11], [12], [13] assist IC designers to analyse thermal induced crack in their designs by simulating stress contour image at the cross-sectional planes of IC chip at different layers. Simulating the stress contour of the IC chips involves the advanced knowledge of different material properties, and they affect stress prediction differently at inter and intra layer level. The material parameter comprising different components, the design variables and process parameters all come together to form an input vector for a corresponding stress contour image. However, there are several challenges when performing stress prediction on IC chips. First, when preparing a design of experiment (DOE) for stress prediction, the number of simulation cases extracted using finite element analysis (FEA) [14], [15], [16] is a problem. In particular, the number of cases for a full factorial dataset is dependent on L levels and P parameters at each layer. From finite element simulation perspective, full factorial DOE at each layer (intra layer) is not feasible. Second, deep generative model can elevate the need for a full factorial DOE using latent space representation. However, label is unknown in the latent space and inverse

modeling of the latent space for stress prediction is not well established. Third, unlike intra layer modeling, different cross-section (inter layer) of the IC chip yield very different stress contour plots. This is due to the heterogeneous integration [17], [18] of complex interfaces between die, underfield (UF) and redistribution layer (RDL). There is no continuity behavior in the image contour at inter layer representation. While each layer can be represented by a deep generative model, it is not practical to train a different model for each layer. Thus, stress prediction is challenging notably due to inverse modeling of stress prediction and having a different model at each layer. We can depict the complexity of inter and intra layer stress prediction in Fig 2. Recent works related to image based stress prediction have mostly used convolutional neural networks and generative adversarial net. Typically, the neural net takes in the shape, boundary and load conditions as images and outputs a stress image. These works are however not related to IC packages and mainly work on dataset that contains homogeneous 2D structures or material fracture. Also, unlike simple 2D structures, the computational cost of obtaining dataset from finite element simulation is much higher for IC package dataset. Current deep generative model cannot easily extend to both intra and inter layer representation. To cope with heterogeneous latent space from inter layer representation, our strategy is to discretize the latent space into Z layers. Thus, we could address both inter and intra class representation, the former which requires a prior knowledge on selecting the number of layers. We propose using an inverse deep generative model for intra layer stress prediction. The model is based on a recently published boundary-decoder net, which consist of an autoencoder and a boundary net. The autoencoder trains a continuous or homogeneous latent space using image contours. The boundary net is responsible for mapping material parameter as vector inputs into the latent space. After training, inverse modeling on the latent space allows us to reconstruct a stress contour image for an unknown vector input. Using finite element simulation, we ran an IC package dataset of 1825 cases for both inter and intra layer. We train the boundary-decoder net using boundary-decoder loss and reconstruction loss. Whereby each iteration, both supervised and unsupervised training is computed on the latent space. To further improve the performance of boundary-

decoder net, we further couple it with deep clustering. As far as we are aware of, this is a novel AI approach which has not been attempted before. Specifically, for each iteration a clustering algorithm such as Kmeans is re-computed on the latent space, before applying deep clustering loss to update the network. As there are no related work, we develop a baseline method known as the AE+KNN to mimic the inter and intra layer representation of our proposed method. We demonstrate on an inhouse IC chip dataset that our proposed deep clustering based boundary-decoder net significantly outperforms baseline method and boundary-decoder net for stress prediction on heterogeneous integrated IC chips for a two die IC design.

We survey works related to mechanical stress image prediction using deep learning [19], [20], [21], [22]. Nie et al [23] introduced image pairs $\pi = \{shape\ image, stress\ image\}$ of 2D structures with 120,960 samples. The input and output images are used to train convolutional neural networks (CNN) layer. Instead of CNN, Jiang et al [19] used generative adversarial net (GAN) to perform stress prediction. The generator provide image pairs to the discriminator to classify whether it resembles the actual dataset. The discriminator in turn trains the generator and the process cycle is repeated. Concurrently, Yang et al [20] used conditional GAN (cGAN) to predict stress image for material composite. cGAN uses a U-net for the generator and PatchGAN for the discriminator. Following [19], they collected a dataset of 2000 image pairs π for training cGAN. Gao et al [22] predict the stress field of crust and rock formation using several CNNs in parallel. Each CNN input is an image, and the output is a X, Y and Z direction stress cube. More recently, Buehler et al [24] combine CycleGAN with transformer architecture to train a stress field prediction model when given a image pairing of image microstructure and stress field. Differently from [24], Wang et al [21] propose future stress field prediction using temporal independent CNN (TI-CNN) and bidirectional long short-term memory (Bi-LSTM) net. The TI-CNN takes microstructure image input but outputs the current feature vector representing stress at one local region. While Bi-LSTM takes past and present feature vector to predict future feature vector. Stress prediction on IC packages is a niche field as it requires cross-discipline domain knowledge to perform an IC package simulation. While many works deploy state-of-the-art deep learning for mechanical stress modeling, their dataset mainly focus on simple 2D structures, unrelated to IC packages. More importantly, they rely on image pairs π , which is not suitable for our case. Our problem requires a multimodal pairing $\phi = \{parameters\ vector, stress\ image\}$ to work. Currently, all the above survey approaches cannot perform stress prediction using ϕ pairing as their deep learning methods cannot solve multimodal cases. Also, stress in heterogeneous IC package is very different from homogeneous 2D structure, crust and rock formation or material fracture pattern.

II. AI DATASET

In this paper, a two dies IC package representative geometry was adopted to demonstrate the methodology of using AI tool to facilitate AI prediction of stresses at different material

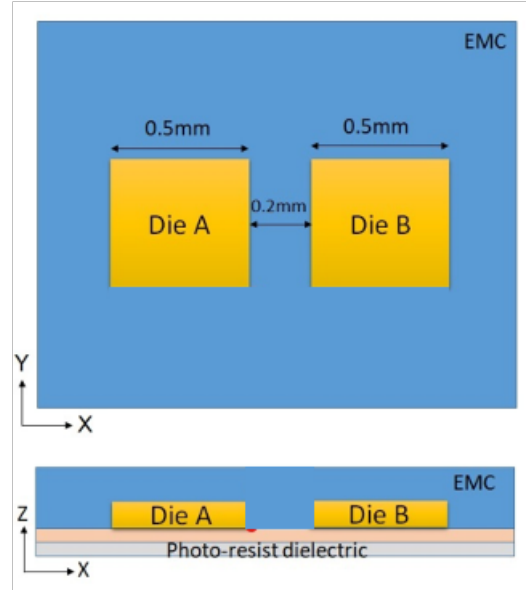


Figure 1: Two dies IC package geometric representation

Table I: DOE for each case using factorial design.

Parameters (P)		Levels (L)
EMC Modulus [GPa]	5~30	5, 11, 17, 23, 30
EMC CTE [ppm/C]	5~20	5, 9, 12, 16, 20
Die Size [mm]	0.5~1.8	0.5, 0.8, 1.2, 1.5, 1.8
Gap between dies [mm]	0.2~1	0.2, 0.4, 0.6, 0.8, 1.0

interfaces inside the package. As shown in Fig. 1, two identical rectangle dies were embedded in the package. Different X-Y, Z-X views of the package structure are presented in Fig.1. Stress (MPa) occurs at the bond between different materials when subjected to thermal cycling (-55deg to 150deg). The X and Y axis refers to the plane while Z and X axis refers to the side view. Silicon (Si) dies are encapsulated by epoxy molding compound (EMC) with overmold on top of dies, i.e. dies are not exposed. Under the Si dies there is the underfill material layer. An RDL layer is at the bottom face of the package.

We focus on the interface between

- 1) EMC and Die - Overmold layer,
- 2) Die and UF - UF layer,
- 3) UF and RDL - RDL layer.

which we call the Overmold, RF and RDL layers, as shown in Fig. 2. Train and test cases are generated based on a full factorial DOE with four variables, i.e. EMC modulus, EMC coefficient of thermal expansion (CTE), die size and gap size between the two dies. Table I lists the DOE of these four variables. 625 cases ($L = 5$, $P = 4$) were generated each layer for $Z = 3$ layers using ANSYS Mechanical for 1825 cases (1500 train and 325 test). The stress result at each mesh point within the FEA model are exported together with the associated coordinates for each case. These results are subsequently used as the training and test data for AI stress predictor model development.

We refer to the example ground truth stress images in Fig 3. using cases corresponding to different parameters (column) and different layer (row). In the overmold layer, there are

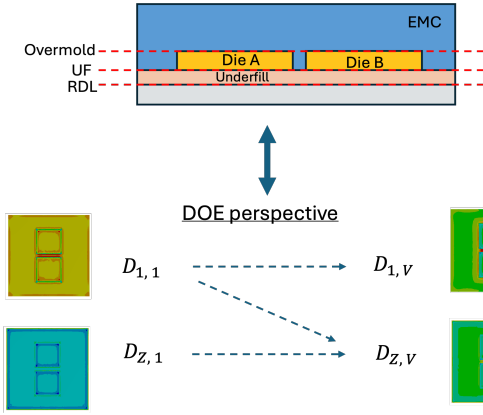


Figure 2: 3D representation of stress prediction, using $D_{1\dots Z, 1\dots V}$ where $Z = 3$ layers and $V = L^P$ cases.

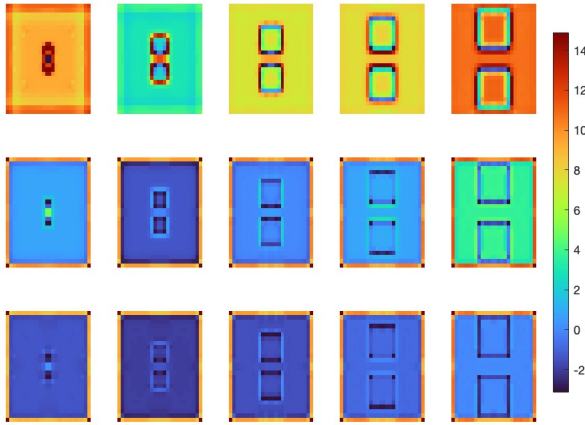


Figure 3: Stress images corresponding to different parameters (column) and at different layers (row).

more stress changes in the images as compared to the UF and RDL layer. We also show the minimum and maximum plot of each layer in Fig 4. These values suggest that the intensity distribution is more consistent for RDL and UF across their respective 625 cases but changes more abruptly for overmold. This is because the parameters in Table 1 (e.g. die size) mainly affects stress at the overmold layer. Parameters such as UF or RDL thickness which may affect stress at UF or RDL layer is not present in our study.

III. AI METHODOLOGY

A. Proposed approach using BD

A recent method known as Boundary Decoder (BD) net [?] as shown in Fig. 5. (yellow path) first maps low dimensional parameters representing boundary conditions, to the latent space z of an autoencoder, and lastly the decoder generates an image. Essentially, BD net behaves like an inverse prediction model. The problem statement of inverse prediction [25] is quoted:

"Given that a regression model can model $1..m$ samples of electrostatic field as $V_{1..m}$ and corresponding

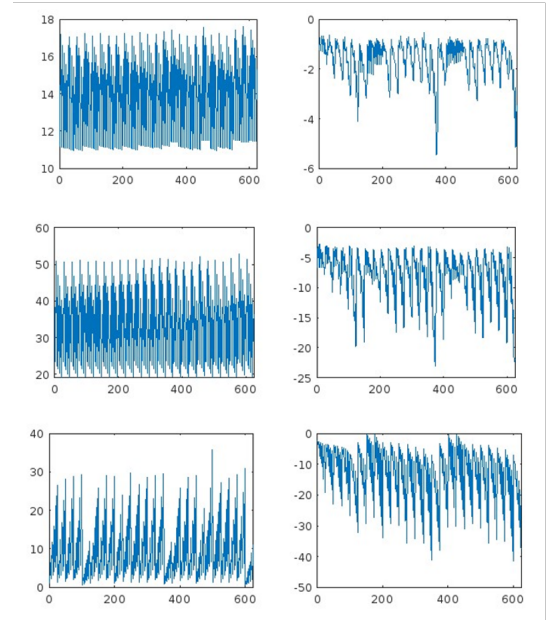


Figure 4: Min and max range for RDL (top row), UF (middle), Overmold (bottom)

boundary condition parameter as output $BC(V_{1..m})$. Inverse prediction then tries to recover input V' when presented with an output $BC(\cdot)$."

Inspired by [25], we treat material parameters as boundary conditions¹ for generating stress image from latent space. This approach requires offline learning by training the BD net architecture using BD loss, L_3 in eqn (1), where y and T are the network image output and the groundtruth image respectively. The input to the boundary net are the material parameters, $vec_{train} = [EMC_E, EMC_{CTE}, Size_{Die}, Size_{Gap}, Layer]$. Using vec_{train} , groundtruth images and L_3 , we update only the weights of the boundary and decoder net.

B. Proposed approach using AE+BD

The abovementioned BD approach may be ill-posed due to mapping input dimensions as low as four parameters to a high dimensional output such as a 26x26 image. In the original BD net [25], it is shown that for capacitor modeling, by jointly training BD with autoencoder (AE), it significantly reduces the error of the generated BD image output. Specifically, we train the full network of Fig 1. using both L_1 and L_3 loss in eqn (1). This has the effect of training the decoder using different objectives, both using reconstruction loss and using BD loss. Since the test case mainly uses BD for output, we regularize the weight update of L_1 using λ_1 for the decoder. In eqn (1), (V, T) and (V', y) refers to the groundtruth and decoder output. We used different terminology to distinguish between BD and AE for the loss variables.

¹We use the naming convention in boundary-decoder net [25]. Strictly speaking, material parameters are not related to boundary conditions found in physics models. Instead, the parameters refer to the physical geometry of the IC chip.

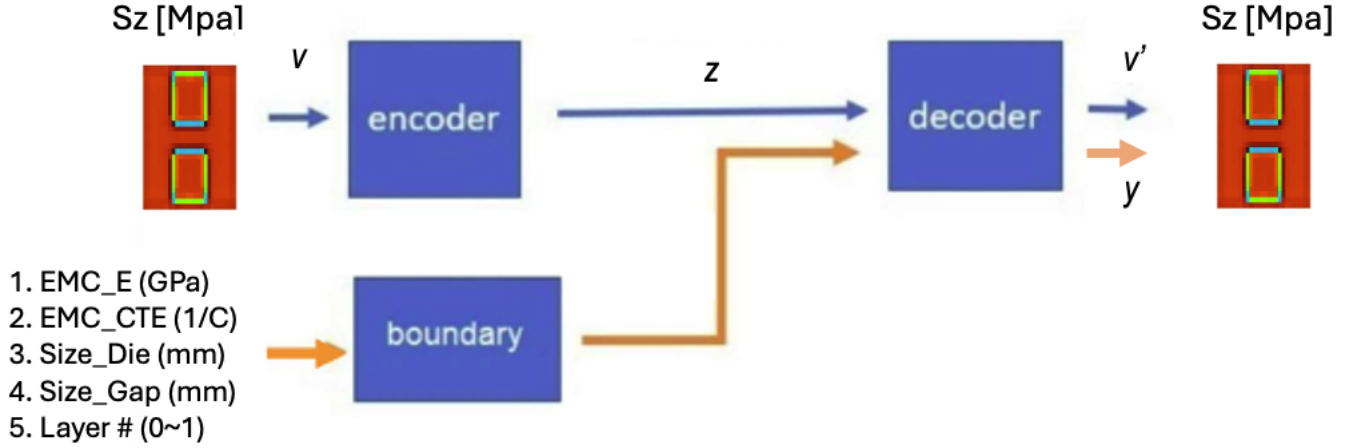


Figure 5: Architecture of Boundary Decoder net

C. Proposed approach using DC+BD

While the L_1 loss of AE improves the performance of BD, we seek to further constraint the latent space by using deep clustering [26]. The goal of deep clustering [26] is to regularize the encoder using statistical method. It actively recomputes *Kmeans* and penalize latent samples for being far apart from their nearest K cluster centers. Specifically, deep clustering constraint all the training images according to their similarities in the latent space. This similarity is determined by 1) the number of clusters predetermined, 2) feature extraction by the encoder and 3) the intensity distribution of the images. The advantage of this approach is that we can train the encoder can better capture the intra layer representation in the latent space. We train the deep clustering based boundary-decoder (DC+BD) net by using all the loss functions found in eqn (1). In eqn (1), η^* refers to the nearest K cluster center and z refers to the encoder output. When training DC+BD, the encoder is trained using L_2 with hyperparameter λ_2 and by L_1 with λ_1 . The decoder is trained by L_1 and L_3 . While the boundary net is trained by L_3 .

$$Loss = \lambda_1 L_1 + \lambda_2 L_2 + L_3$$

$$= \left\{ -\frac{\lambda_1}{2} (V - V')^2 \right\} + \left\{ -\frac{\lambda_2}{2} (\eta^* - z)^2 \right\} + \left\{ -\frac{1}{2} (T - y)^2 \right\} \quad (1)$$

D. Baseline approach using AE+KNN

We also introduce a baseline for stress image prediction, using AE and K-Nearest-Neighbor (KNN). The objective is found in eqn (2). Using training images, we train an AE to represent images in the latent space. This is stored in the form of an array $latent_{train}$, corresponding to their input vector counterparts vec_{train} . For an unseen test input vector, vec_{test} is compared against vec_{train} using KNN to select an optimal training sample vec_{train}^* . Then, the optimal vec_{train}^* samples which corresponds to its $latent_{train}^*$ sample counterpart, is in turn fed to the decoder to reconstruct an image, V' . The autoencoder is trained using L_1 loss in eqn (1) to update

Table II: Comparison of Boundary-Decoder (BD) variants vs baseline

	train error	test error	train time
AE+KNN(baseline)	-	0.1589±0.0186	30~40s
BD (proposed)	0.1424±0.0069	0.1437±0.0014	8~25s
AE+BD (proposed)	0.1416±0.0031	0.1409±0.0074	25~50s
DC+BD (proposed)	0.1441±0.0056	0.1309±0.0019	400~600s

the weights of the encoder and decoder. The cons of this approach is that both AE and KNN training are disjointed and the method requires a large training dataset to make up for the the lack of offline learning involved. The pro is that this method is fast to compute, apart from requiring a large memory storage for $latent_{train}$.

$$vec_{train}^* = KNN(vec_{test}, vec_{train})$$

$$latent_{train}^* = F_{vec \rightarrow latent} \{vec_{train}^*\} \quad (2)$$

$$V' = F_{latent \rightarrow decoder} \{latent_{train}^*\}$$

IV. EXPERIMENTS

A. Training and testing error comparison

We make a comparison of our proposed Boundary-Decoder variants (BD, AE+BD, DC+BD) with baseline (AE+KNN) in Table II and Fig. 6. Each scatter point refers to the sum-of-square-difference error between groundtruth and generated image for a particular iteration termination run. We rerun each method for at least 3-5 times from initial random weights with different iteration termination runs (8000, 12000, 22000, 42000) to show their scatter plots, along with their optimal linear regression lines (using “fitlm” in Matlab). In the train error graph in Fig. 6, we observe that BD and AE+BD have slightly on-par regression lines across, while DC+BD leads early on but converge similarly to the other two methods. AE+KNN is not valid for this comparison. We support this finding in Table II, where all variants of BD have similar average train error after 42000 iterations.

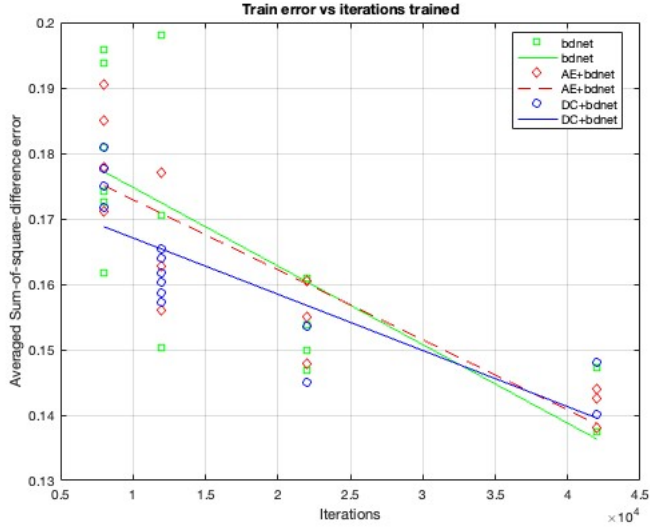


Figure 6: Scatter points and regression lines for 1500 train samples.

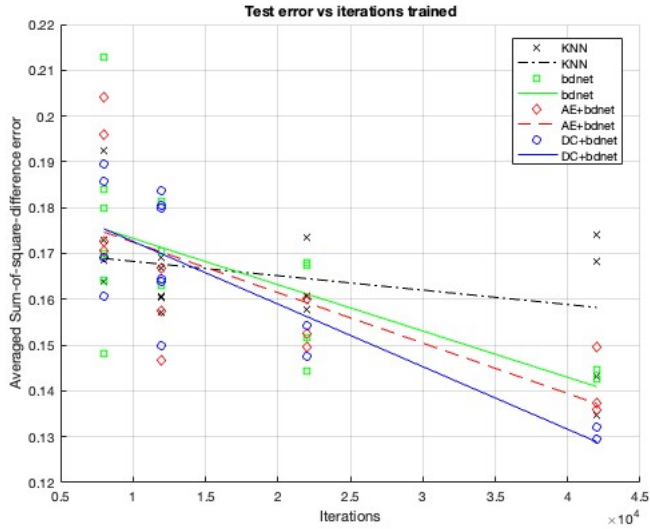


Figure 7: Scatter points and regression lines for 375 test samples.

When we look at the test error in Fig 7, it is evident that baseline AE+KNN appears to have limited error reduction, while all variant of BD outperforms AE+KNN after training for at least 12000 iterations. Notably, DC+BD outperforms all the methods by a large margin at 42000 iterations. Table II numerically shows AE+BD and DC+BD outperform BD by 1.9% and 8.9%. Moreover, DC+BD leads AE+KNN by 17.6%. This suggest that while the train error of the supervised trained BD is on par with AE+BD and DC+BD, BD generalize poorer than DC+BD when tested on unseen samples. We attribute this performance gain by the unsupervised training of AE+BD and DC+BD. In particular, DC+BD achieved this by using a more compact latent space known as deep clustering, to minimize intra-cluster variation.

In terms of computational speed in Table II, BD is the fastest, followed by AE+BD, AE+KNN and lastly DC+BD.

The expensive cost in DC+BD is mainly due to the load of recomputing *Kmeans* on all the training samples in the latent space each training iteration.

B. Visual comparison of proposed methods

Fig 8. to Fig. 10. are using larger die sizes at the upper end of 0.5~1.8 in Table I. We can visualize the generated train (top row) and test (bottom row) images of BD, AE+BD and DC+BD at different layers. For overmold, there is distinct contrast between the foreground and background. This is because the material parameters in Table I are directly affecting the geometry in the overmold layer. The parameter effect is less significant for the UF layer and RDL layer as they are further away from the two dies. The physical location of the dies is illustrated in Fig 2. In terms of the metric error using sum-of-square-difference (ssd), we observed that DC-BD mostly outperforms the two other variants of BD for all the layers. AE+BD appears to be poorer than BD. We also note for RDL, it is much harder for the 3 methods to capture stress as the intensity difference between foreground and background is not significant.

For the small die size comparison in Fig 11. to Fig. 13, we observe all variants of BD appear to have image artifact in the generated images for the overmold layer. We suspect this is could be due to limited training samples. Overall for small dies comparison, we observe that BD visually outperforms both AE+BD and DC+BD.

V. CONCLUSION

We introduce stress prediction for a 2 dies IC chip. To cope with different material parameters and different interface layers of the IC chip, we represent stress prediction as a latent space problem. The problem with latent space analysis is that the samples are unlabeled. To overcome this, we use boundary-decoder net which jointly trains labels (continuous value) with image in the latent space. The labels of the boundary-decoder net refer to material parameters. To generate an image, the latent sample of the label is fed into the decoder. To further improve the decoder capability, we enhance the training using deep clustering. We developed a stress prediction dataset of 1825 samples where a comparison is made between baseline and proposed variants of boundary-decoder. We demonstrate that boundary-decoder is successful at performing stress prediction on our inhouse dataset. In future, we would like to explore how stress prediction can be generalized to varying number of dies.

VI. ACKNOWLEDGEMENT

This work is supported by "Predictive Package Integrity and Reliability for Multi Chiplet Heterogeneous Integration Products"

REFERENCES

- [1] S. S. Iyer, "Heterogeneous integration for performance and scaling," *IEEE Transactions on Components, Packaging and Manufacturing Technology*, vol. 6, no. 7, pp. 973–982, 2016.

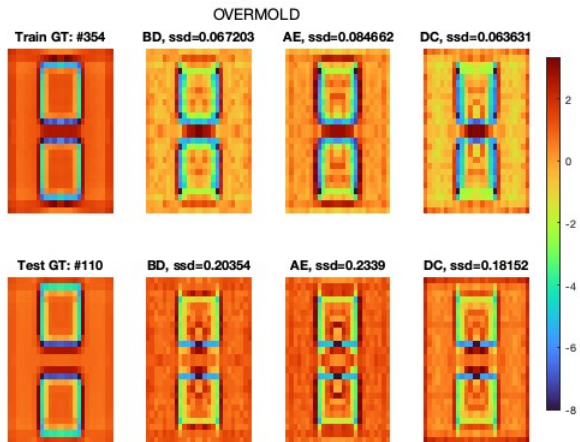


Figure 8: Large die size for overmold layer

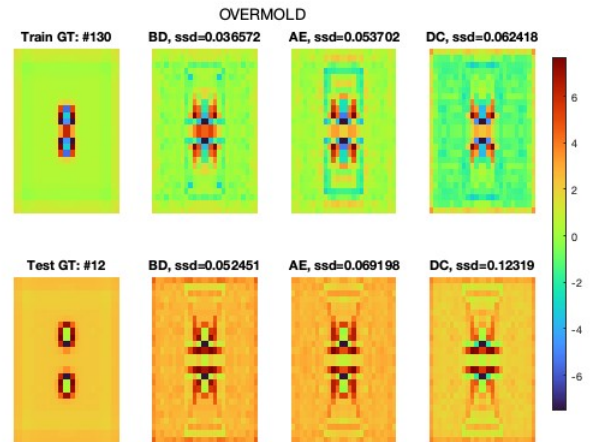


Figure 11: Small die size for overmold layer

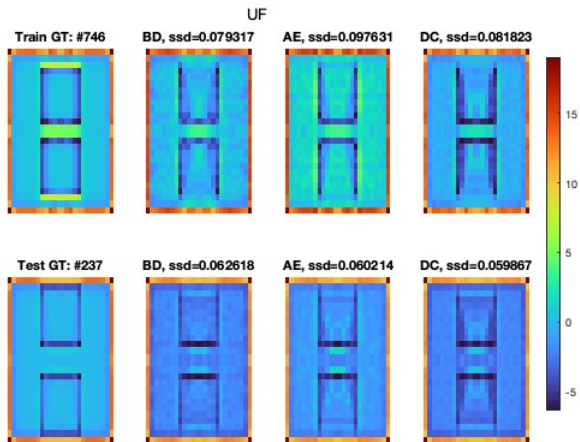


Figure 9: Large die size for UF layer

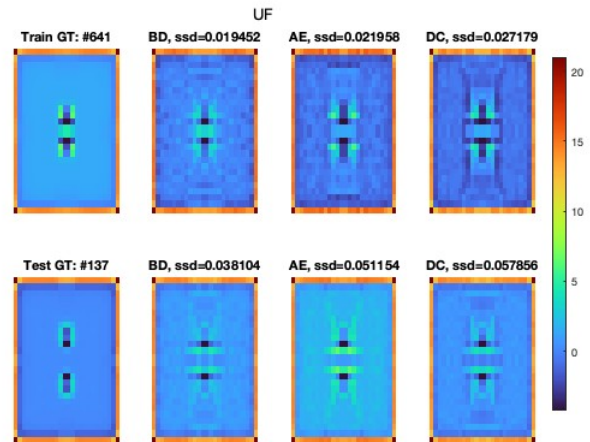


Figure 12: Small die size for UF layer

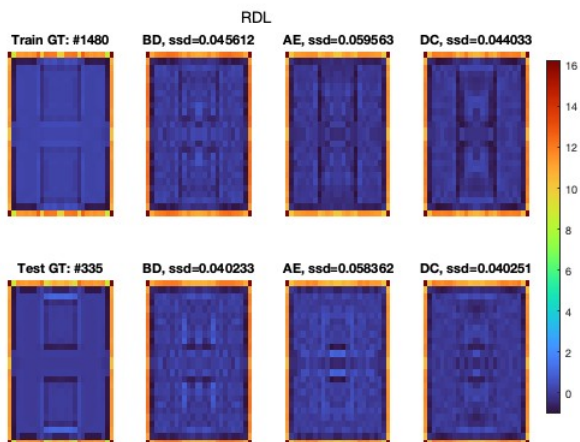


Figure 10: Large die size for RDL layer

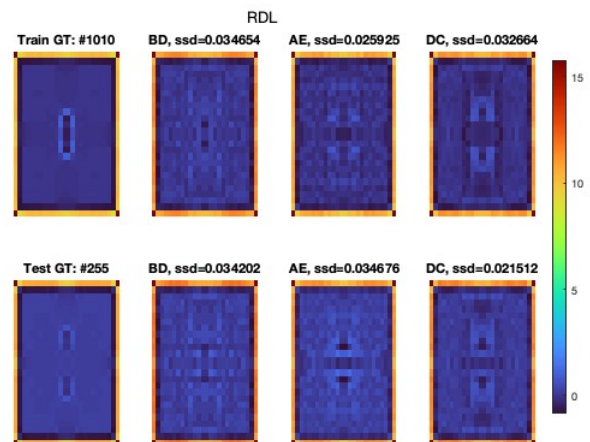


Figure 13: Small die size for RDL layer

- [2] J. H. Lau, "Recent advances and trends in advanced packaging," *IEEE Transactions on Components, Packaging and Manufacturing Technology*, vol. 12, no. 2, pp. 228–252, 2022.
- [3] R. Mahajan, R. Nair, V. Wakharkar, J. Swan, J. Tang, and G. Vandentop, "Emerging directions for packaging technologies," *Intel Technology Journal*, vol. 6, no. 2, 2002.
- [4] J. H. Lau, *Chiplet design and heterogeneous integration packaging*. Springer, 2023.
- [5] R. C. Blish, "Temperature cycling and thermal shock failure rate modeling," in *1997 IEEE international reliability physics symposium proceedings. 35th annual*. IEEE, 1997, pp. 110–117.
- [6] J. H. Lau, "Thermal fatigue life prediction of flip chip solder joints by fracture mechanics method," *Engineering Fracture Mechanics*, vol. 45, no. 5, pp. 643–654, 1993.
- [7] J. H. Pang, D. Chong, and T. Low, "Thermal cycling analysis of flip-chip solder joint reliability," *IEEE Transactions on components and packaging technologies*, vol. 24, no. 4, pp. 705–712, 2001.
- [8] L. Niu, D. Yang, and M. Zhao, "Study on thermo-mechanical reliability of embedded chip during thermal cycle loading," in *2009 International Conference on Electronic Packaging Technology & High Density Packaging*. IEEE, 2009, pp. 1229–1232.
- [9] M.-Y. Tsai, C. J. Hsu, and C. O. Wang, "Investigation of thermomechanical behaviors of flip chip bga packages during manufacturing process and thermal cycling," *IEEE Transactions on Components and Packaging Technologies*, vol. 27, no. 3, pp. 568–576, 2004.
- [10] J. Zhang, M. O. Bloomfield, J.-Q. Lu, R. J. Gutmann, and T. S. Cale, "Modeling thermal stresses in 3-d ic interwafer interconnects," *IEEE transactions on semiconductor manufacturing*, vol. 19, no. 4, pp. 437–448, 2006.
- [11] S. Park, H. Lee, B. Sammakia, and K. Raghunathan, "Predictive model for optimized design parameters in flip-chip packages and assemblies," *IEEE Transactions on Components and Packaging Technologies*, vol. 30, no. 2, pp. 294–301, 2007.
- [12] S.-J. Hsieh, "Artificial neural networks and statistical modeling for electronic stress prediction using thermal profiling," *IEEE transactions on electronics packaging manufacturing*, vol. 27, no. 1, pp. 49–58, 2004.
- [13] E. Suhir, "Predictive analytical thermal stress modeling in electronics and photonics," 2009.
- [14] B. Vandeveld, A. Ivankovic, B. Debecker, M. Lofrano, K. Vanstreels, W. Guo, V. Cherman, M. Gonzalez, G. Van der Plas, I. De Wolf *et al.*, "Chip-package interaction in 3d stacked ic packages using finite element modelling," *Microelectronics Reliability*, vol. 54, no. 6-7, pp. 1200–1205, 2014.
- [15] Y. Shen, L. Zhang, W. Zhu, J. Zhou, and X. Fan, "Finite-element analysis and experimental test for a capped-die flip-chip package design," *IEEE Transactions on Components, Packaging and Manufacturing Technology*, vol. 6, no. 9, pp. 1308–1316, 2016.
- [16] A. B. Jørgensen, S. Munk-Nielsen, and C. Uhrenfeldt, "Overview of digital design and finite-element analysis in modern power electronic packaging," *IEEE Transactions on Power Electronics*, vol. 35, no. 10, pp. 10 892–10 905, 2020.
- [17] H.-J. Lee, R. Mahajan, F. Sheikh, R. Nagisetty, and M. Deo, "Multidie integration using advanced packaging technologies," in *2020 IEEE Custom Integrated Circuits Conference (CICC)*. IEEE, 2020, pp. 1–7.
- [18] D. Lu and C. Wong, *Materials for advanced packaging*. Springer, 2009, vol. 181.
- [19] H. Jiang, Z. Nie, R. Yeo, A. B. Farimani, and L. B. Kara, "Stressgan: A generative deep learning model for two-dimensional stress distribution prediction," *Journal of Applied Mechanics*, vol. 88, no. 5, p. 051005, 2021.
- [20] Z. Yang, C.-H. Yu, and M. J. Buehler, "Deep learning model to predict complex stress and strain fields in hierarchical composites," *Science Advances*, vol. 7, no. 15, p. eabd7416, 2021.
- [21] Y. Wang, D. Oyen, W. Guo, A. Mehta, C. B. Scott, N. Panda, M. G. Fernández-Godino, G. Srinivasan, and X. Yue, "Stressnet-deep learning to predict stress with fracture propagation in brittle materials," *Npj Materials Degradation*, vol. 5, no. 1, p. 6, 2021.
- [22] W. Gao, X. Lu, Y. Peng, and L. Wu, "A deep learning approach replacing the finite difference method for in situ stress prediction," *IEEE Access*, vol. 8, pp. 44 063–44 074, 2020.
- [23] Z. Nie, H. Jiang, and L. B. Kara, "Stress field prediction in cantilevered structures using convolutional neural networks," *Journal of Computing and Information Science in Engineering*, vol. 20, no. 1, p. 011002, 2020.
- [24] E. L. Buehler and M. J. Buehler, "End-to-end prediction of multimaterial stress fields and fracture patterns using cycle-consistent adversarial and transformer neural networks," *Biomedical Engineering Advances*, vol. 4, p. 100038, 2022. [Online]. Available: <https://www.sciencedirect.com/science/article/pii/S2667099222000147>
- [25] K.-L. Lim, R. Dutta, and M. Rotaru, "Boundary-decoder network for inverse prediction of capacitor electrostatic analysis," 2024. [Online]. Available: <https://arxiv.org/abs/2412.00113>
- [26] K.-L. Lim, "Deep clustering using adversarial net based clustering loss," 2025. [Online]. Available: <https://arxiv.org/abs/2412.08933>